Supporting information for:

Electron Flow through Nitrotyrosinate in *Pseudomonas aeruginosa* Azurin

Jeffrey J. Warren, Nadia Herrera, Michael G. Hill, Jay R. Winkler and Harry B. Gray*

Beckman Institute
and
Division of Chemistry and Chemical Engineering
California Institute of Technology
Pasadena CA 91125
USA

Department of Chemistry
Occidental College
Los Angeles CA 90041
USA

hbgray@caltech.edu

Contents

1. Protein Modification Protocols

1.1 Tyrosine Nitration.

Azurin proteins containing a single, surface exposed, tyrosine are readily nitrated using a slightly modified literature procedure.[S1] A septum-capped Schlenk flask was charged with 30 mL of approximately 250 μM solution of azurin in 25 mM sodium phosphate buffer at pH 8. The solution was deoxygenated with several gentle pump-argon backfill cycles. A freshly prepared solution (19 mL) of 1% v/v tetranitromethane (Sigma-Aldrich) in absolute ethanol was added dropwise to the protein solution. The solution was stirred for 3 hours, changing from the characteristic blue color of azurin to a deep green. The protein solution was concentrated using ultrafiltration and desalted into 10 mM Tris buffer at pH 9 using a PD-10 column (GE Healthcare). The protein was FPLC purified using a Q-HP column (GE Healthcare) and eluting with a NaCl gradient. Purity was assessed using UV-vis spectroscopy and mass spectrometry. Isolated yields of ≥ 90% are based upon comparison of total protein by UV-vis before and after nitration ($\varepsilon_{630}(Cu^{II\text{-}azurin}) = 5600\ M^{-1}\ cm^{-1}$).

1.2 Ruthenium Labeling.

Ru-labeling of azurin was performed using a slightly modified literature procedure.[S2] NO_2YOH-modified azurin was exchanged into 300 mM $NaHCO_3$ buffer to give a final concentration of 300 μM (10 mL, ~50 mg). Freshly dissolved Ru(2,2′-bipyridine)$_2CO_3$[S3] (1.1 equiv. in 300 mM $NaHCO_3$) was added and the resulting purple solution was allowed to react for several hours overnight at room temperature to yield a green solution. The protein solution was

(S1) Lee, J. C.; Langen, R.; Hummel, P. A.; Gray, H. B.; Winkler, J. R. *Proc. Natl. Acad. Sci. U.S.A.* **2004,** *101*, 16466-16471.
(S2) Faham, S.; Day, M. W.; Connick, W. B.; Crane, B. R.; Di, B., Angel J.; Schaefer, W. P.; Rees, D. C.; Gray, H. B. *Acta Cryst. D* **1999,** *55*, 379-385.
(S3) Johnson, E. C.; Sullivan, B. P.; Salmon, D. J.; Adeyemi, S. A.; Meyer, T. J. *Inorg. Chem.* **1978,** *17*, 2211-2215.

concentrated using ultrafiltration and desalted into 10 mM Tris buffer + 1 M NaCl at pH 8 using a PD-10 column (GE Healthcare). Modified and unmodified azurin were separated using a Hi-Trap Chelating column (GE Healthcare). Replacement of the water molecule coordinated to Ru(2,2′-bipyridine)(HisX) (X = 107, 124, 126) was achieved by exchanging the protein into 500 mM imidazole, 100 mM NaCl and 1 mM $CuSO_4$ at pH 7.5. The protein was incubated a room temperature for 3-5 days and purified using a Q-HP column (GE Healthcare) and eluting with a NaCl gradient. Proteins were stored in the above imidazole buffer at 4°C and desalted into the appropriate buffer for other experiments. Proteins were characterized using UV-vis spectroscopy and mass spectrometry.

2. UV-vis characterization of NO_2YO^- and Ru-modified azurins.

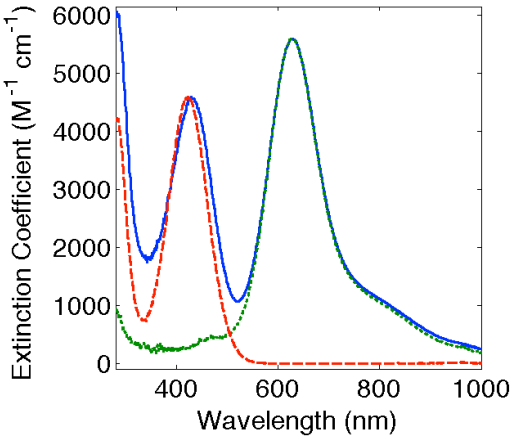

Figure S1. UV-vis spectra of 3-nitrotyrosinate (NO_2YO^-, Sigma-Aldrich) (red – – –), Cu^{II} All Phe *P. aeruginosa* azurin (green •••), and H126NO_2YO^- Cu^{II} azurin (blue ——). All components are in 50 mM sodium phosphate + 50 mM NaCl, pH 8.5.

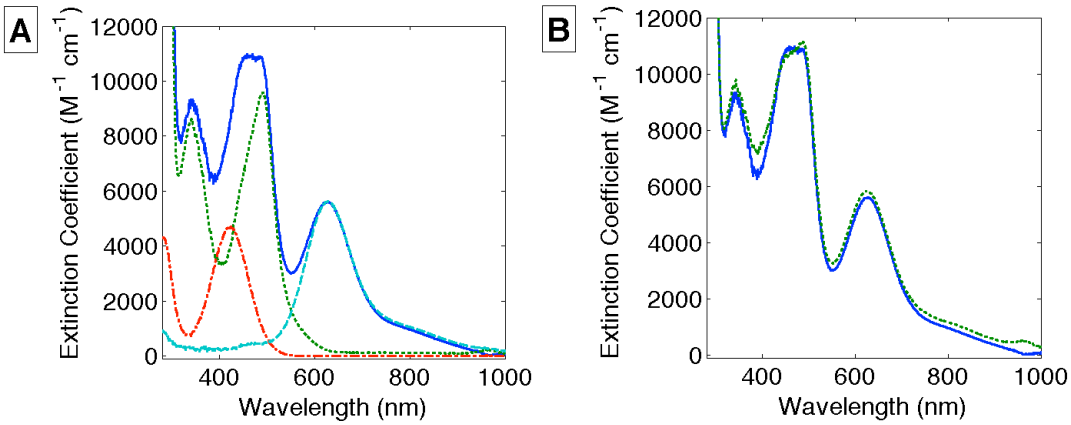

Figure S2. (A) UV-vis spectra of 3-nitrotyrosinate (NO_2YO^-, Sigma-Aldrich) (red – • –), Cu^{II} All Phe *P. aeruginosa* azurin (cyan – – –), Ru(2,2′-bipyridine)$_2$(imidazole)$_2Cl_2$ (green •••) and Ru H126NO_2YO^- Cu^{II} azurin (blue ——). (B) Comparison of Ru H126NO_2YO^- Cu^{II} azurin (blue — –) and the linear combination of the component spectra shown in (A) (green •••). All components are in 50 mM sodium phosphate + 50 mM NaCl, pH 8.5.

3. Mass spec of Ru(2,2´-bipyridine)(imidzaole)(HisX)-NO_2YOH-modifed azurins.

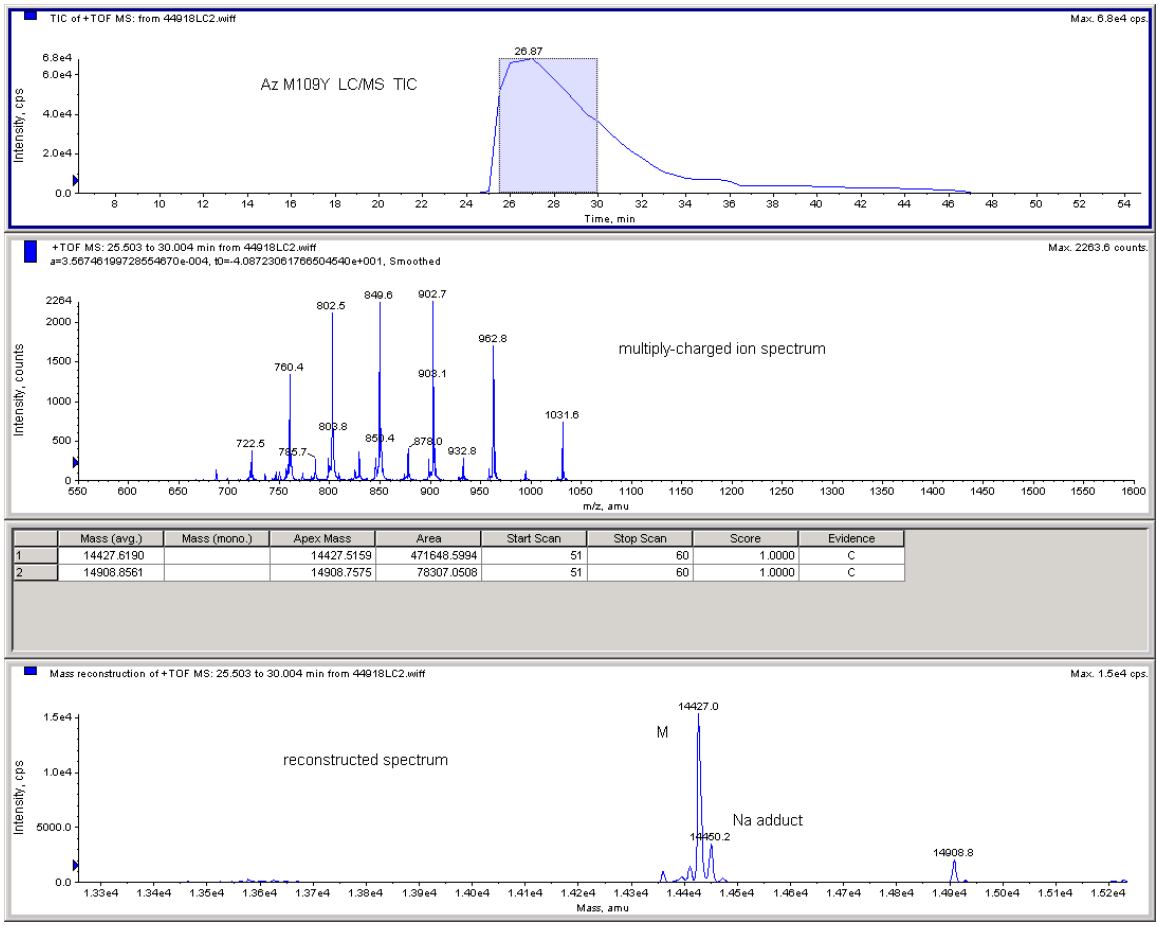

	Mass (avg.)	Mass (mono.)	Apex Mass	Area	Start Scan	Stop Scan	Score	Evidence
1	14427.6190		14427.5159	471648.5994	51	60	1.0000	C
2	14908.8561		14908.7575	78307.0508	51	60	1.0000	C

Figure S3. Mass spec for RuH107NO_2YOH109 azurin. Azurin loses its Cu^{2+} ion in the mass spec. The molecular weight (MW) of the un-nitrated protein is 13907 g mol^{-1}. The protein with nitration of YOH109 has MW = 13953 g mol^{-1}. Addition of Ru^{II}(2,2´-bipyridine)(imidazole) (481.5 g mol^{-1}) gives a final MW of 14434 g mol^{-1}. The observed mass is 14427 g mol^{-1}.

Protein Sequence: A E C S V D I Q G N D Q M Q F N T N A I T V D K S C K Q F T V N L S H P G N L P K N V M G H N F V L S T A A D M Q G V V T D G M A S G L D K D F L K P D D S R V I A Q T K L I G S G E K D S V T F D V S K L K E G E **H** F **Y** F F C T F P G H S A L M K G T L T L K

*NO_2-modified Y and Ru-modified H are in bold.

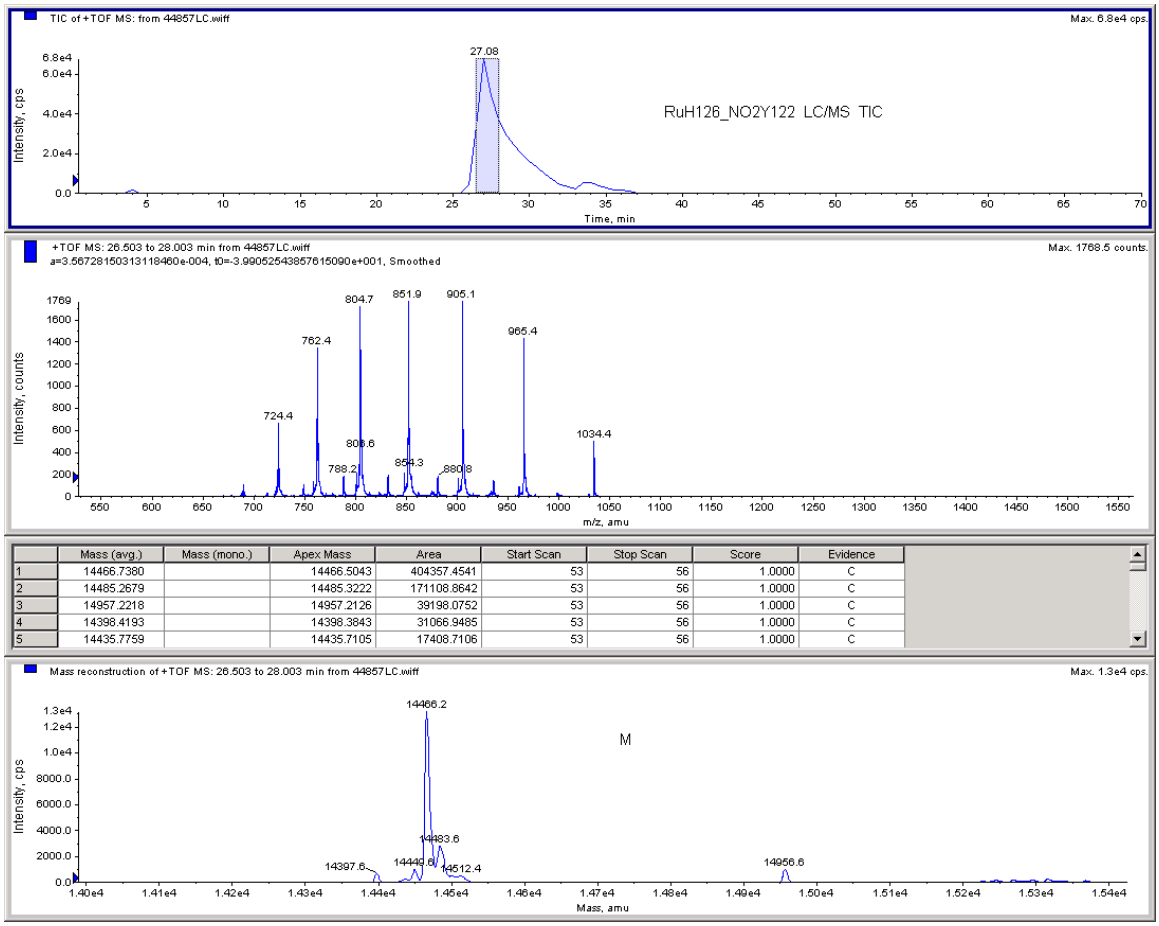

	Mass (avg.)	Mass (mono.)	Apex Mass	Area	Start Scan	Stop Scan	Score	Evidence
1	14466.7380		14466.5043	404357.4541	53	56	1.0000	C
2	14485.2679		14485.3222	171108.8642	53	56	1.0000	C
3	14957.2218		14957.2126	39198.0752	53	56	1.0000	C
4	14398.4193		14398.3843	31066.9485	53	56	1.0000	C
5	14435.7759		14435.7105	17408.7106	53	56	1.0000	C

Figure S4. Mass spec for RuH126NO_2YOH122 azurin. Azurin loses its Cu^{2+} ion in the mass spec. The molecular weight (MW) of the un-nitrated protein is 13937 g mol^{-1}. The protein with nitration of YOH109 has MW = 13983 g mol^{-1}. Addition of Ru^{II}(2,2′-bipyridine)(imidazole) (481.5 g mol^{-1}) gives a final MW of 14464 g mol^{-1}. The observed mass is 14466 g mol^{-1}.

Protein Sequence: A E C S V D I Q G N D Q M Q F N T N A I T V D K S C K Q F T V N L S H P G N L P K N V M G H N F V L S T A A D M Q G V V T D G M A S G L D K D F L K P D D S R V I A Q T K L I G S G E K D S V T F D V S K L K E G E Q F M F F C T F P G H S A L M **Y** G T L **H** L K

*NO_2-modified Y and Ru-modified H are in bold.

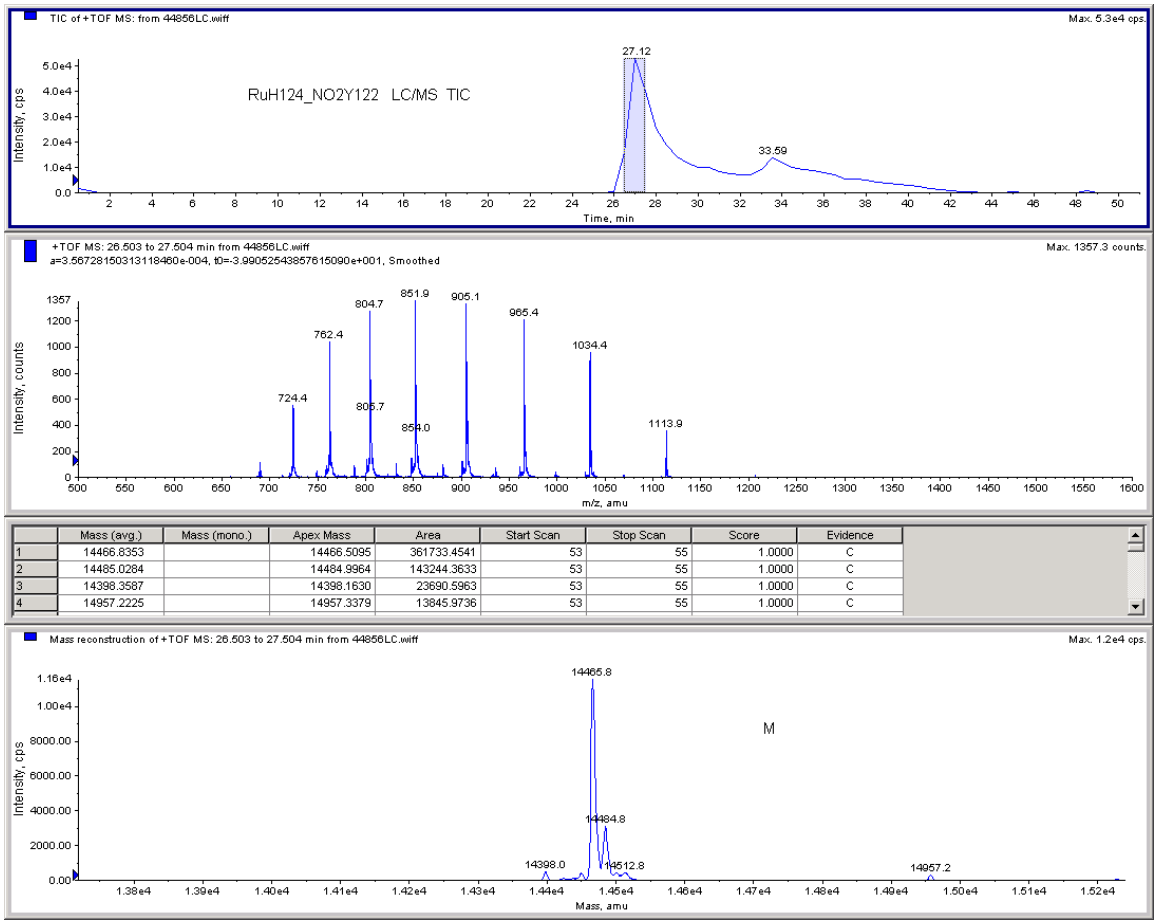

	Mass (avg.)	Mass (mono.)	Apex Mass	Area	Start Scan	Stop Scan	Score	Evidence
1	14466.8353		14466.5095	361733.4541	53	55	1.0000	C
2	14485.0284		14484.9964	143244.3633	53	55	1.0000	C
3	14398.3587		14398.1630	23690.5963	53	55	1.0000	C
4	14957.2225		14957.3379	13845.9736	53	55	1.0000	C

Figure S5. Mass spec for RuH124NO_2YOH122 azurin. Azurin loses its Cu^{2+} ion in the mass spec. The molecular weight (MW) of the un-nitrated protein is 13937 g mol^{-1}. The protein with nitration of YOH109 has MW = 13983 g mol^{-1}. Addition of Ru^{II}(2,2′-bipyridine)(imidazole) (481.5 g mol^{-1}) gives a final MW of 14464 g mol^{-1}. The observed mass is 14466 g mol^{-1}.

Protein Sequence: A E C S V D I Q G N D Q M Q F N T N A I T V D K S C K Q F T V N L S H P G N L P K N V M G H N F V L S T A A D M Q G V V T D G M A S G L D K D F L K P D D S R V I A Q T K L I G S G E K D S V T F D V S K L K E G E Q F M F F C T F P G H S A L M **Y** G **H** L T L K

*NO_2-modified Y and Ru-modified H are in bold.

4. Azurin structures and ET distance determination.

The H126NO_2YO$^-$ and H124NO_2YO$^-$ azurins could only be crystallized in the absence of Ru-label. The distances required for analysis with semiclassical theory had to be estimated by other means. ET distances for RuH126NO_2YO$^-$ and RuH124NO_2YO$^-$ were estimated using the models shown in Figure S6 and S7, respectively. Cα overlays were generated using the "align" function in PyMOL. Although the Re^I-label in the models is different from the Ru^{II}-label used in the current study, we believe that these models provide reasonable estimates of the true ET distances. The effects of different ET distance formulations on hopping maps are described below.

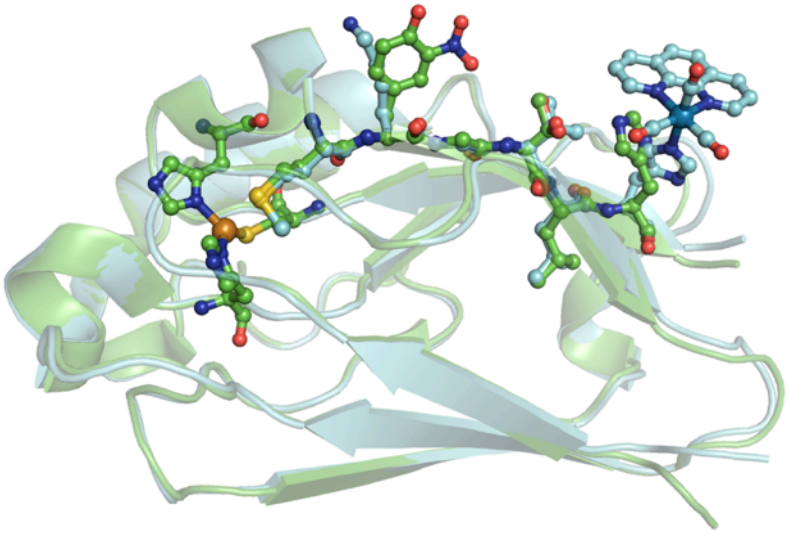

Figure S6. C-α overlay of H126NO_2YOH azurin (PDB 4HIP) with $Re(CO)_3$(4,7-dimethyl-phenanthroline)H126-azurin (PDB 3IBO). RMS = 0.311.

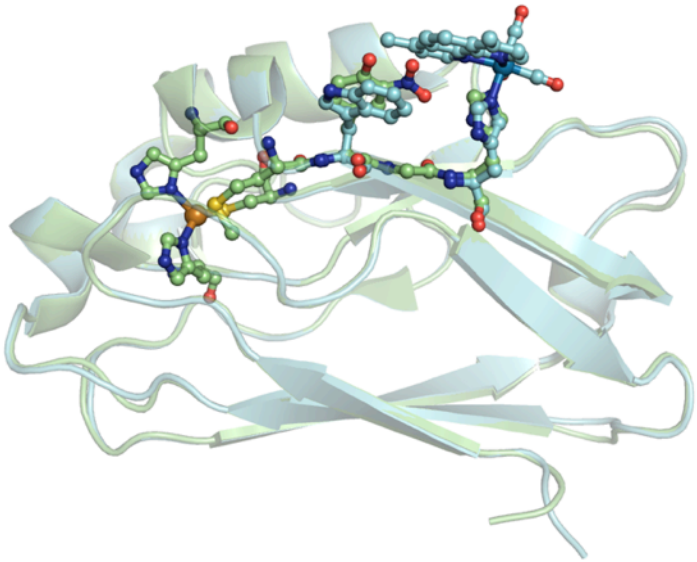

Figure S7. C-α overlay of H124NO_2YOH122 azurin (PDB 4HHW) with $Re(CO)_3$(4,7-dimethyl-phenanthroline)H124W122 azurin (PDB 2I7O). RMS = 0.249.

5. Effects of reorganization energy and electronic coupling on hopping advantage maps.

The hopping advantage maps in the main text used our empirical ET parameters for tunneling in azurin (λ = 0.8 eV, β = 1.1 Å^{-1}). Presented in the following sections are a series of maps that explore the effects associated with varying those parameters. In each map the driving forces and electronic coupling at close contact are fixed (as noted in the captions).

The conclusions from these maps follow those in the main text. Unsurprisingly, the greatest hopping advantage is achieved for driving force optimized ET ($-\Delta G° = \lambda$) and when the distance for each tunneling step is minimized. Maps with smaller β have a shallower change in electronic coupling (H_{AB}) as a function of distance, resulting in fewer cofactor arrangements that could provide a hopping advantage. Hopping in these better-coupled systems is less advantageous than in more weakly coupled systems. It follows that when H_{AB} changes more as a function of distance (larger β) single-step ET becomes less likely and a greater hopping advantage is possible. A critical conclusion here is that breaking a large donor-acceptor distance into shorter tunneling steps produces the greatest hopping *advantage*, but this does not necessarily provide any information about the absolute tunneling times when comparing systems with different cofactor arrangements.

5.1 Hopping advantage maps with variable reorganization energy (λ)

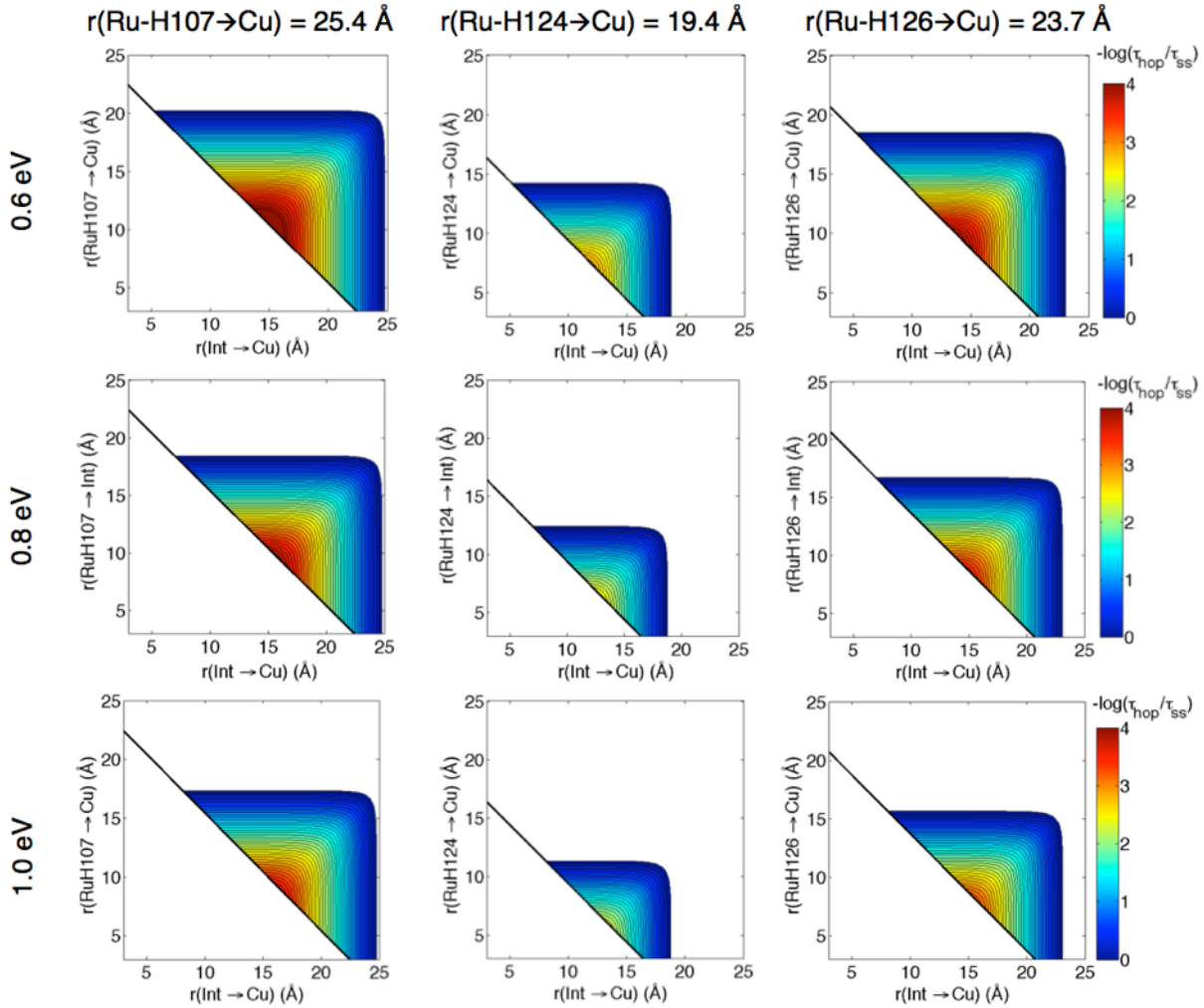

Figure S8. Hopping advantage maps for a two-step ET system (Cu^{I}→Int→Ru^{III}) in each of three azurins. In each map the overall driving force $-\Delta G°(\text{Int}\rightarrow Ru^{III})$ is 0 eV and $-\Delta G°(Cu^{I}\rightarrow Ru^{III})$ is 0.7 eV, T is 298 K, the distance decay constant (β) is 1.1 $Å^{-1}$, and the close-contact coupling element (H_{AB}^{0}) is 186 cm^{-1}. τ_{hop} is the calculated hopping time and τ_{ss} is the calculated single-step tunneling time. The contour lines are plotted at 0.1 log unit intervals. The reorganization energies (λ) are indicated at the left. The center row is the same as in Figure 1 of the main text.

5.2 Hopping advantage maps with variable electronic coupling (β)

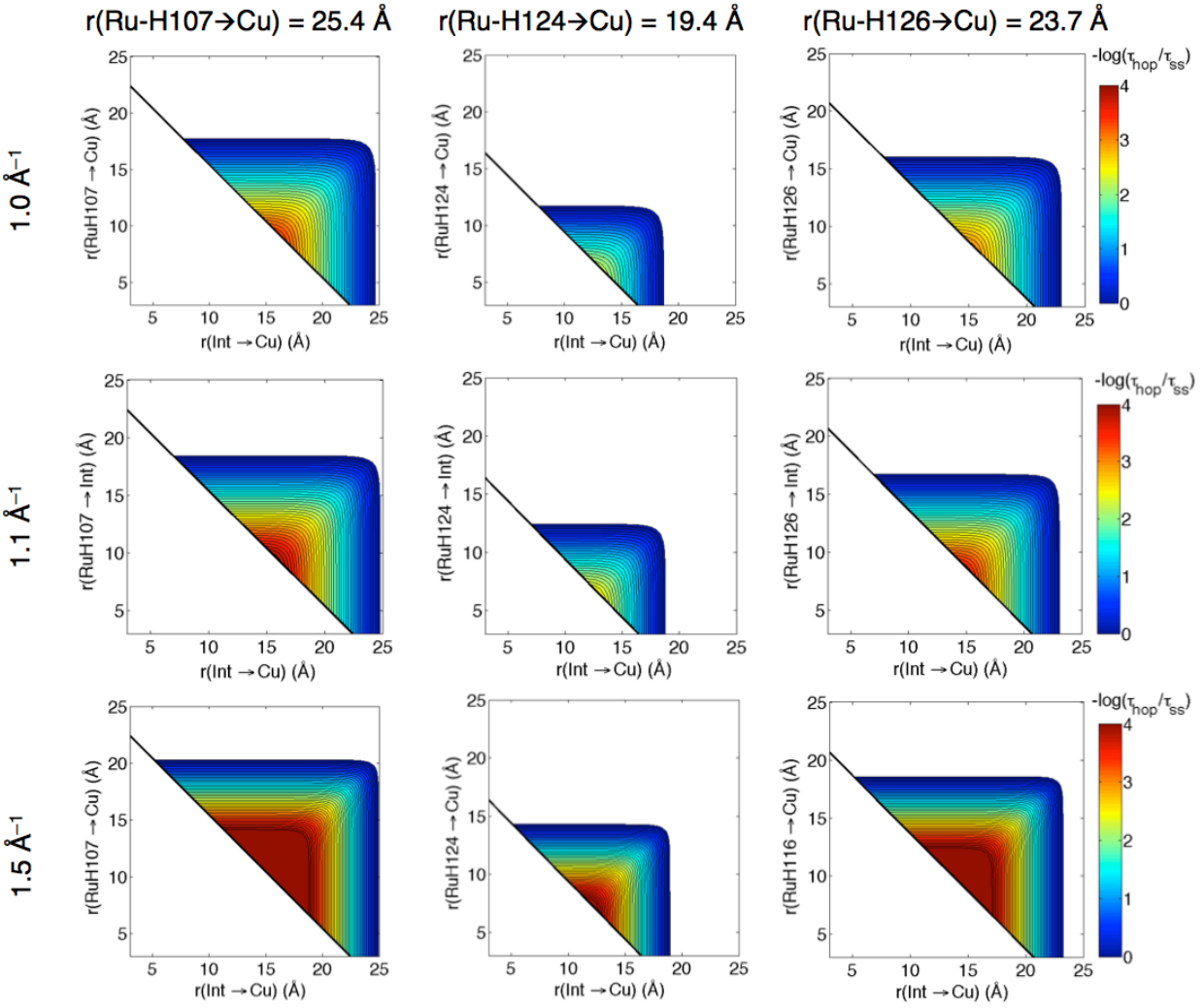

Figure S9. Hopping advantage maps for a two-step ET system (Cu^{I}→Int→Ru^{III}) in each of three azurins. In each map the overall driving force $-\Delta G°$(Int→Ru^{III}) is 0 eV and $-\Delta G°$(Cu^{I}→Ru^{III}) is 0.7 eV, T is 298 K, the reorganization energies (λ) is 0.7 eV, and the close-contact coupling element (H_{AB}^{0}) is 186 cm^{-1}. τ_{hop} is the calculated hopping time and τ_{ss} is the calculated single-step tunneling time. The contour lines are plotted at 0.1 log unit intervals. The distance decay constants (β) are indicated at left. The center row is the same as in Figure 1 of the main text.

6. Center-to-center versus edge-to-edge distances for hopping maps.

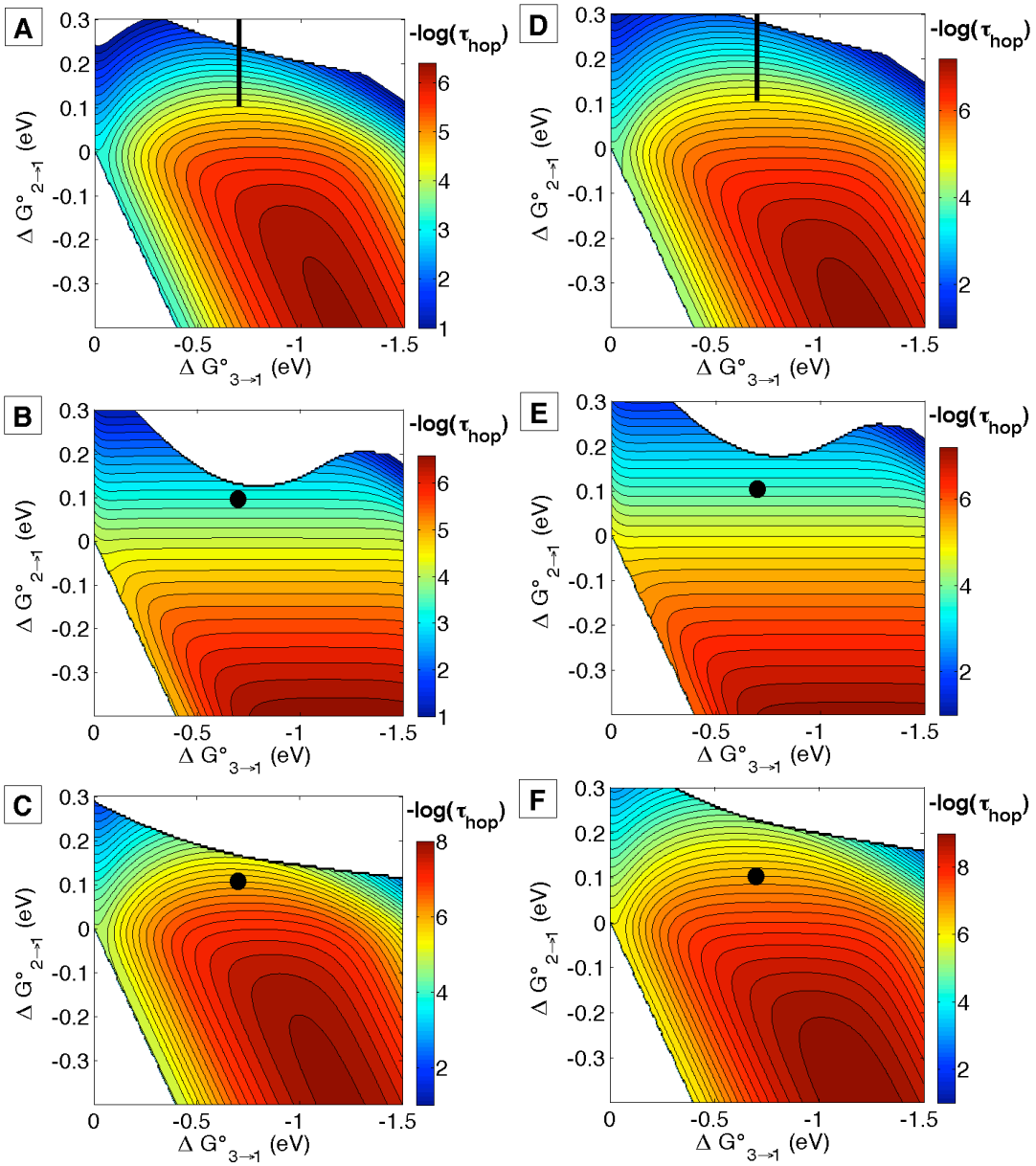

Figure S10. Hopping maps for NO_2YO^--substituted azurins: (A), (B), and (C) are as in the main text. Maps (D), (E), and (F) are made using the distances between the closest aromatic carbon in NO_2YO^- and the Ru^{II} (r_1) or Cu^{II} (r_2). The carbon in NO_2YO^- used for the distance formulation is given in the subscript. The distances are: (A), (D) RuH107NO_2YO^-109 with $r_{1\text{-}C3}$ = 10.4 (11.4), $r_{2\text{-}C1}$ = 14.9 (16.7), r_3 = 25.4 (25.4) Å; (B), (E) RuH126NO_2YO^-122 with $r_{1\text{-}C3}$ = 13.1 (14.2), $r_{2\text{-}C6}$ = 11.1 (13.3), r_3 = 23.7 (23.7) Å; and (C), (F) RuH124NO_2YO^-122 with $r_{1\text{-}C3}$ = 6.7 (7.8), $r_{2\text{-}C2}$ = 10.9 (13.3), r_3 = 19.4 (19.4) Å. In all maps λ = 0.8 eV, β = 1.1 $Å^{-1}$, T = 298 K and H_{AB}^0 = 186 cm^{-1}. The subscripts 1, 2, and 3 refer to the Ru^{III}, NO_2YO^-, and Cu^I, respectively. The contour lines are plotted at 0.2 log unit intervals. The black dots (or black bar in (A) and (D)) are at the driving forces given in the text.

Table S1. Comparison of hopping rate constants for different distance formulations.

	k_{hop} [a]	$k_{hop(calc)}$ [b]	$k_{hop(calc)}$ [d]
Ru(H107)	$(7.7 \pm 0.5) \times 10^3$	8.7×10^2 [c]	5.0×10^3 [c]
Ru(H126)	$(6.0 \pm 0.5) \times 10^3$	2.3×10^3	7.8×10^3
Ru(H124)	$(3.0 \pm 0.5) \times 10^5$	1.3×10^6	7.1×10^6

[a] $k_{hop} = k_{hopping}$ [b] $k_{hop(calc)}$ are from the hopping maps shown in A, B and C (center-to-center distances). [c] Calculated with $\Delta G°(NO_2YO^-109 \rightarrow Ru^{III}) = 0.2$ eV. [d] $k_{hop(calc)}$ are from the hopping maps shown in D, E and F (edge-to-edge distances).

Hopping maps constructed using center-to-center distances (from the main text) and using edge-to-edge distances are shown in Figure S10. The ET distances for each formulation are not dramatically different, so the shapes of the maps do not change very much. Using edge-to-edge distances results in shorter tunneling steps, so the calculated rate constants increase by about a factor of 5. The calculated hopping rate constants are in better agreement with experiment for $RuH107NO_2YO^-109$ and $RuH126NO_2YO^-122$, but show poorer agreement with experiment for $RuH124NO_2YO^-122$.

As noted in the main text, subtle changes in ET distance, reorganization energy, and electronic coupling can have marked effects on predictions of semiclassical ET theory. As such, semiclassical ET theory is usually accurate within an order of magnitude for single step ET. We show here that semiclassical ET theory provides good predictive power and design criteria for hopping systems, but that predictive power is limited by the accuracy of the many ET parameters for each step.

7. Effects of variable λ and β on predictions from hopping maps.

We also analyzed the effects of changing λ and β (using center-to-center ET distances) on the predictions from hopping maps. The results are tabulated in Table S2 and the individual hopping maps are shown in Figure S11-S16. We varied λ between 0.6 and 1.0 eV and β between 1.0 and 1.5 $Å^{-1}$. In both cases, the range of parameter values is reasonable for biological systems.

Analysis of the hopping maps generated from varying λ and β support our use of or empirical values (0.8 eV and 1.1 $Å^{-1}$, respectively) for tunneling via redox partners on a single β-strand in azurin. Varying λ between 0.6 and 1.0 eV affects predicted hopping rate constants by less than a factor of 5, except for Ru126NO_2YO$^-$122. In that case, rates for ET through the non-optimally arranged cofactors (with a large distance for the uphill first step) is more sensitive to changes in λ. Hopping is not predicted in poorly coupled systems (β = 1.5 $Å^{-1}$), in accord with our observation that ET in Ru-modified proteins is largely described by β = 1.1 ± 0.1 $Å^{-1}$.

Table S2. Calculated hopping rate constants for Ru-labled NO_2YO$^-$ azurins.[a]

	Ru(H107)[b]	Ru(H126)	Ru(H124)
	(7.7 ± 0.5) × 10^3	**(6.0 ± 0.5) × 10^3**	**(3.0 ± 0.5) × 10^5**
λ = 0.6 eV	3.1 × 10^2	1.8 × 10^4	1.3 × 10^6
λ = 0.8 eV	**8.7 × 10^2**	**2.3 × 10^3**	**1.3 × 10^6**
λ = 1.0 eV	4.1 × 10^2	NA	2.8 × 10^5
β = 1.0 $Å^{-1}$	3.0 × 10^3	7.2 × 10^3	2.6 × 10^6
β = 1.1 $Å^{-1}$	**8.7 × 10^2**	**2.3 × 10^3**	**1.3 × 10^6**
β = 1.5 $Å^{-1}$	NA	NA	NA

[a] All rate constants are s^{-1}. Values in bold are those given in the main text. All other values are taken from the hopping maps in Figures S11-S16. The observed rate constants for ET in each system are given in the second row. [b] All values are calculated with $\Delta G°$(NO_2YO$^-$109→Ru^{III}) = 0.2 eV

7.1 Maps for RuH107NO_2YO$^-$109 azurin

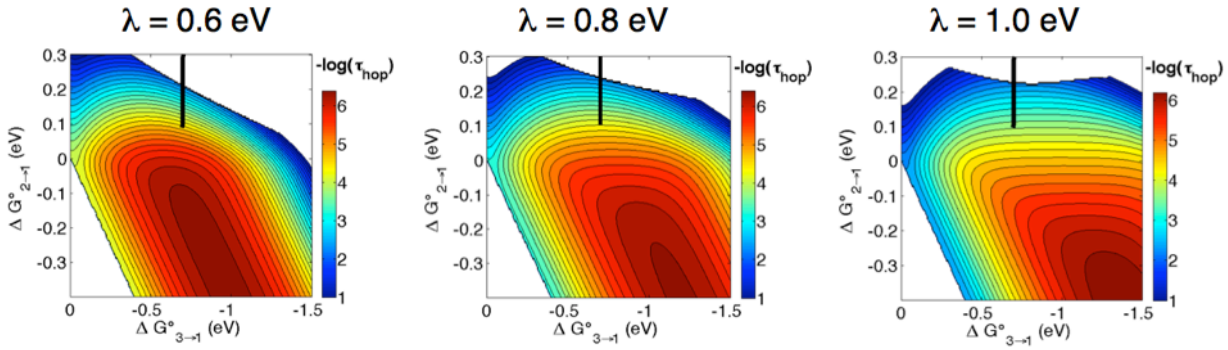

Figure S11. Hopping maps for RuH107NO_2YO$^-$109 azurin showing the effect of varying the reorganization energy (λ) between 0.6 and 1.0 eV (at top). The maps were constructed with r_1 = 11.5, r_2 = 15.5, r_3 = 25.4 Å. In all maps β = 1.1 Å^{-1}, T = 298 K and $H_{AB}{}^0$ = 186 cm^{-1}. The subscripts 1, 2, and 3 refer to Ru^{III}, NO_2YO^- and Cu^I respectively. The contour lines are plotted at 0.2 log unit intervals. The black bar represents the driving forces given in the main text.

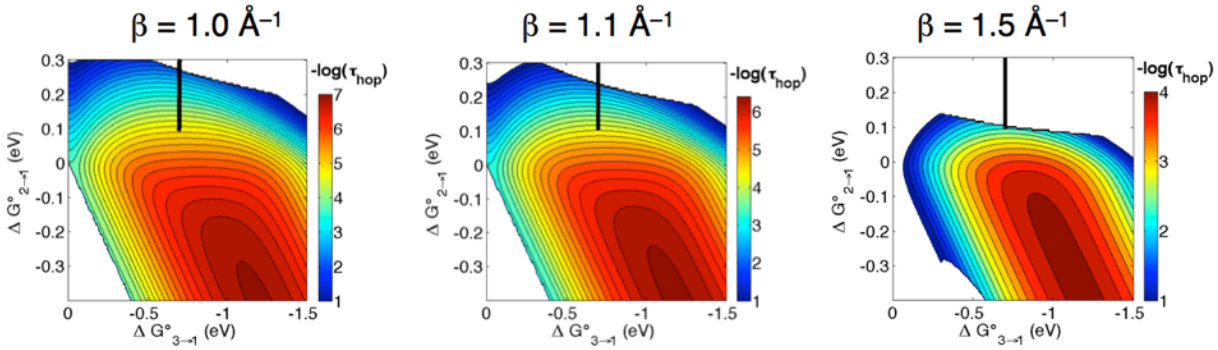

Figure S12. Hopping maps for RuH107NO_2YO$^-$109 azurin showing the effect of varying the electronic coupling decay constant (β) between 1.0 and 1.5 Å^{-1} (at top). The maps were constructed with r_1 = 11.5, r_2 = 15.5, r_3 = 25.4 Å. In all maps the reorganization energy (λ) is 0.8 eV, T = 298 K and $H_{AB}{}^0$ = 186 cm^{-1}. The subscripts 1, 2, and 3 refer to Ru^{III}, NO_2YO^- and Cu^I respectively. The contour lines are plotted at 0.2 log unit intervals. The black bar represents the driving forces given in the main text.

7.2 Maps for RuH126NO_2YO$^-$122 azurin

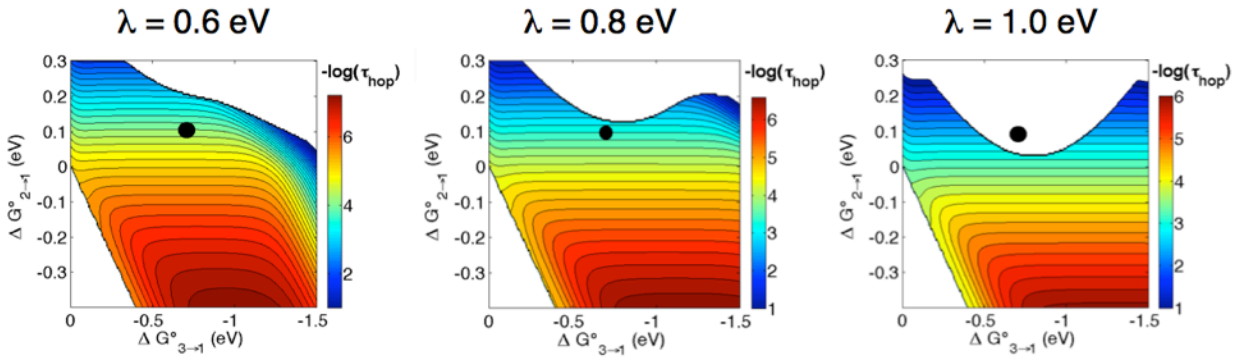

Figure S13. Hopping maps for RuH126NO_2YO$^-$109 azurin illustrating the effect of varying the reorganization energy (λ) between 0.6 and 1.0 eV (at top). The maps were constructed with r_1 = 14.3, r_2 = 11.5, r_3 = 23.7 Å. In all maps β = 1.1 Å^{-1}, T = 298 K and H_{AB}^0 = 186 cm^{-1}. The subscripts 1, 2, and 3 refer to Ru^{III}, NO_2YO^- and Cu^I respectively. The contour lines are plotted at 0.2 log unit intervals. The black bar represents the driving forces given in the main text.

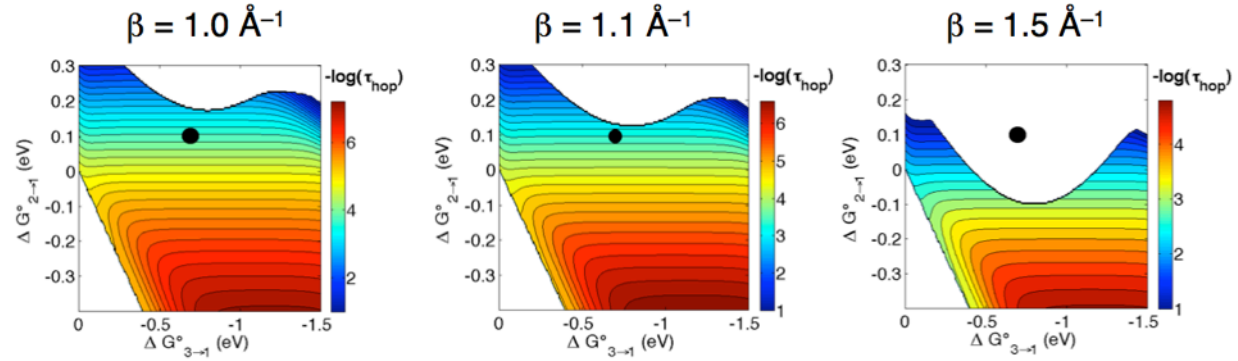

Figure S14. Hopping maps for RuH126NO_2YO$^-$109 azurin showing the effect of varying the electronic coupling decay constant (β) between 1.0 and 1.5 Å^{-1} (at top). The maps were constructed with r_1 = 14.3, r_2 = 11.5, r_3 = 23.7 Å. In all maps the reorganization energy (λ) is 0.8 eV, T = 298 K and H_{AB}^0 = 186 cm^{-1}. The subscripts 1, 2, and 3 refer to Ru^{III}, NO_2YO^- and Cu^I respectively. The contour lines are plotted at 0.2 log unit intervals. The black bar represents the driving forces given in the main text.

7.3 Maps for RuH124NO_2YO$^-$122 azurin

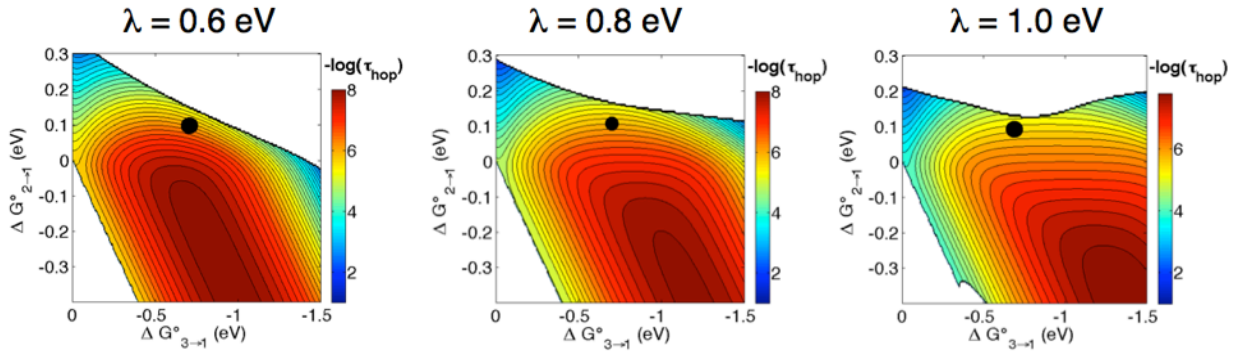

Figure S15. Hopping maps for RuH124NO_2YO$^-$109 azurin illustrating the effect of varying the reorganization energy (λ) between 0.6 and 1.0 eV (at top). The maps were constructed with r_1 = 8.3, r_2 = 12.3, r_3 = 19.4 Å. In all maps β = 1.1 Å^{-1}, T = 298 K and $H_{AB}{}^0$ = 186 cm^{-1}. The subscripts 1, 2, and 3 refer to Ru^{III}, NO_2YO^- and Cu^I respectively. The contour lines are plotted at 0.2 log unit intervals. The black bar represents the driving forces given in the main text.

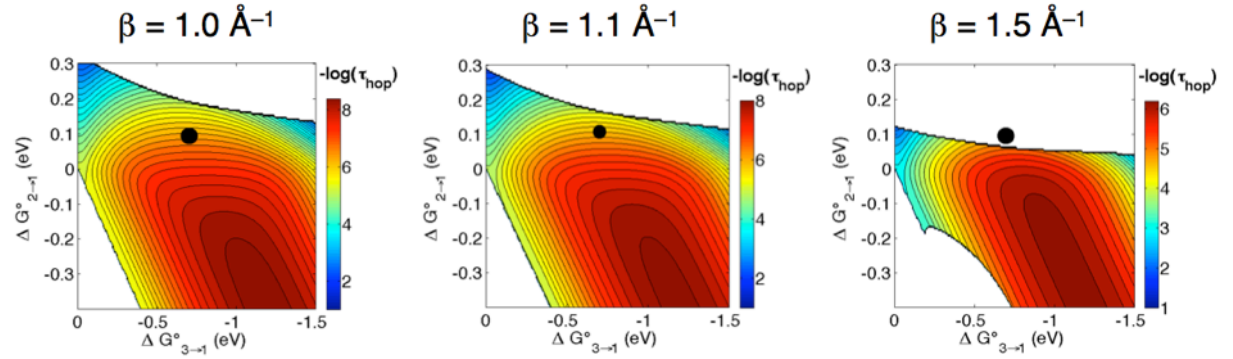

Figure S16. Hopping maps for RuH124NO_2YO$^-$109 azurin showing the effect of varying the electronic coupling decay constant (β) between 1.0 and 1.5 Å^{-1} (at top). The maps were constructed with r_1 = 8.3, r_2 = 12.3, r_3 = 19.4 Å. In all maps the reorganization energy (λ) is 0.8 eV, T = 298 K and $H_{AB}{}^0$ = 186 cm^{-1}. The subscripts 1, 2, and 3 refer to Ru^{III}, NO_2YO^- and Cu^I respectively. The contour lines are plotted at 0.2 log unit intervals. The black bar represents the driving forces given in the main text.